Acta Crystallographica Section D
Biological Crystallography
ISSN 0907-4449

Crystallographic analysis of potent and selective factor Xa inhibitors complexed to bovine trypsin

Marc Whitlow,* Damain O. Arnaiz, Brad O. Buckman, David D. Davey, Brain Griedel, William J. Guilford, Sunil K. Koovakkat, Amy Liang, Raju Mohan, Gary B. Phillips, Marian Seto, Kenneth J. Shaw, Wei Xu, Zuchun Zhao, David R. Light and Michael M. Morrissey

Berlex Biosciences, 15049 San Pablo Avenue, PO Box 4099, Richmond, California 94804, USA

Correspondence e-mail: marc_whitlow@berlex.com

Received 12 March 1999
Accepted 27 May 1999

PDB References: trypsin–2-aminobenzimidazole complex, 1qa0; trypsin–2-{5-[amino(imino)methyl]-2-hydroxyphenoxy}-6-[3-(4,5-dihydro-1*H*-imidazol-2-yl)phenoxy]pyridine-4-carboxylic acid complex, 1qbn; trypsin–7-[(6-{[1-(1-iminoethyl)piperidin-4-yl]oxy}-2-methyl-1*H*-benzimidazol-1-yl)methyl]-naphthalene-2-carboximidamide complex, 1qbo; trypsin–1-(2-{5-[amino(imino)methyl]-2-hydroxyphenoxy}-6-[3-(4,5-dihydro-1-methyl-1*H*-imidazol-2-yl)phenoxy]pyridin-4-yl)piperidine-3-carboxylic acid complex, 1qb1; trypsin–3,3′-[3,5-difluoro-4-methyl-2,6-pyridinediylbis(oxy)] bis(benzenecarboximidamide) complex, 1qb6; trypsin–7-[(2-{[1-(1-iminoethyl)piperidin-4-yl]oxy}-9*H*-carbozol-9-yl)methyl]naphthalene-2-carboximidamide complex, 1qb9.

Factor Xa is a serine protease which activates thrombin (factor IIa) and plays a key regulatory role in the blood-coagulation cascade. Factor Xa is, therefore, an important target for the design of anti-thrombotics. Both factor Xa and thrombin share sequence and structural homology with trypsin. As part of a factor Xa inhibitor-design program, a number of factor Xa inhibitors were crystallographically studied complexed to bovine trypsin. The structures of one diaryl benzimidazole, one diaryl carbazole and three diaryloxypyridines are described. All five compounds bind to trypsin in an extended conformation, with an amidinoaryl group in the S1 pocket and a second basic/hydrophobic moiety bound in the S4 pocket. These binding modes all bear a resemblance to the reported binding mode of DX-9065a in bovine trypsin and human factor Xa.

1. Introduction

In the development of factor Xa inhibitors for the treatment and prevention of thrombotic disease, it is important for the inhibitors to have specificity with respect to other serine proteases such as trypsin. Both factor Xa and trypsin are serine proteases which hydrolyze the C-terminal peptide bond to positively charged amino acids. Owing to the large quantities of trypsin in the gut, any potential drug that has high affinity for trypsin will have low bioavailability and could affect a patient's digestion. The sequence identity between human trypsin and the serine-protease domain of human factor Xa is 36%. Trypsin has a much broader substrate specificity than factor Xa, which converts the zymogen prothrombin (factor II) to thrombin (factor IIa) as part of the prothrombinase complex of factor Xa, factor Va, phospholipid and calcium. Thrombin is the final enzymatic product in the blood-coagulation cascade and converts fibrinogen to fibrin. In addition to the serine-protease domain, factor Xa has a γ-carboxyglutamic acid (Gla) domain and two domains similar to epidermal growth factor (EGF-like domains). The Gla domain, with its 11 Gla residues, helps anchor factor Xa in the phospholipid membrane, and the two EGF-like domains have been shown to interact with factor Va in the prothrombinase complex.

Factor Xa is the point at which the intrinsic and extrinsic pathways of the blood-coagulation cascade converge. Zymogen factor X is converted to factor Xa by the factor XIa–factor VIIIa complex in the intrinsic pathway or by the factor VIIa–tissue-factor complex in the extrinsic pathway (Davie *et al.*, 1991). The extrinsic pathway is activated by the exposure of tissue factor during tissue damage. The intrinsic pathway, as the name implies, accounts for blood's intrinsic ability to clot and is activated by negatively charged phospholipids.

So why develop a factor Xa inhibitor? Factor Xa inhibitors reduce fibrin clot formation by reducing the levels of thrombin and subsequently fibrin. There are a number of problems with the currently available anticoagulant therapies. Heparin, which inhibits thrombin, requires antithrombin III as a cofactor. Heparin and all of its various forms have low bioavailability and thus must be injected. It has a narrow therapeutic range, requiring monitoring, and bleeding complications are one of the more serious side effects. Coumarin (warfarin), which inhibits vitamin K production, has a delayed onset of action. Monitoring is required owing to variable dose responses of different patients, and vitamin K levels are affected by a patient's diet. A comparison of thrombin inhibitors with factor Xa inhibitors in a canine model of acute coronary artery thrombosis suggests that factor Xa inhibitors would make a better anticoagulant (Sitko *et al.*, 1992). Unlike a factor Xa inhibitor, a thrombin inhibitor does not prevent the formation of more thrombin by the prothrombinase complex at the site of vascular injury. In addition, thrombin itself has some anticoagulant functions.

Padmanabhan *et al.* (1993) have solved the crystal structure of des 1–44 factor Xa. Several attempts were made to produce inhibitor complexes, but these failed owing to the blocked active site in this crystal form. Recently, Brandstetter *et al.* (1996) and Kamata *et al.* (1998) have produced and solved the structures of factor Xa–inhibitor complexes. To date, we have been unable to produce crystals of factor Xa complexed to one of our inhibitors. In order to gain some insight into the binding and conformation of our potent, selective and orally active non-peptide inhibitors we prepared bovine trypsin complexes. The X-ray crystal structures of bovine trypsin complexed with five factor Xa inhibitors will be described. All of these compounds bind in an extended conformation with an amidinoaryl group in the S1 pocket and a second basic/hydrophobic moiety bound in the S4 pocket. These binding modes all bear a resemblance to the reported binding mode of DX-9065A in bovine trypsin (Stubbs *et al.*, 1995) and in human factor Xa (Brandstetter *et al.*, 1996).

2. Experimental

2.1. Compound synthesis

The synthesis and structure–activity relationships of 7-[(6-{[1-(1-iminoethyl)piperidin-4-yl]oxy}-2-methyl-1*H*-benz-imidazol-1-yl)methyl]naphthalene-2-carboximidamide (I; Griedel, *et al.* 1998); 7-[(2-{[1-(1-iminoethyl)piperidin-4-yl]-oxy}-9*H*-carbozol-9-yl)methyl]naphthalene-2-carboximidamide (II; Arnaiz *et al.*, 1998); 3,3′-[3,5-difluoro-4-methyl-2,6-pyridinediylbis(oxy)] bis(benzenecarboximidamide) (III; Phillips *et al.*, 1998, 1999); 2-{5-[amino(imino)methyl]-2-hydroxyphenoxy}-6-[3-(4,5-dihydro-1*H*-imidazol-2-yl)phenoxy]pyridine-4-carboxylic acid (IV; Phillips *et al.*, 1998, 1999), and 1-(2-{5-[amino(imino)methyl]-2-hydroxyphenoxy}-6-[3-(4,5-dihydro-1-methyl-1*H*-imidazol-2-yl)phenoxy]pyridin-4-yl)piperidine-3-carboxylic acid (V; Phillips *et al.*, 1998) have previously been described.

2.2. Inhibition constants (K_i) for factor Xa and trypsin

Commercial purified serine proteases, human factor Xa (Enzyme Research Laboratories, Inc., South Bend, IN, USA) and bovine cationic trypsin (Boehringer Mannheim Corp., Indianapolis, IN, USA) were assayed in 150 m*M* NaCl, 2.5 m*M* $CaCl_2$, 50 m*M* Tris–HCl pH 7.5 and 0.1% PEG 6000 in a final volume of 200 µl in 96-well microtiter plates at room temperature with Chromogenix substrates (Kabi Pharmacia Hepar Inc., Franklin, OH, USA). The initial cleavage rates of the peptide *p*-nitroanilide by the enzyme were determined by measuring the rate of the absorbance change at 405 nm in a ThermoMax microplate reader (Molecular Devices Corp., Sunnyvale, CA; Lottenberg *et al.*, 1981). The final concentrations of enzyme and substrate were 1 n*M* factor Xa with 164 µ*M* S-2222 and 16 n*M* trypsin with 40 µ*M* S-2266. Inhibition mechanism is competitive; therefore, a substrate concentration equal to K_m was used to assay varying concentrations of the inhibitor to determime the K_i. K_i values of very potent inhibitors (<3 n*M*) were determined by fitting data obtained at 0.3 and 1 n*M* factor Xa to a modified Morrison equation (Morrison, 1969) to correct for the proportion of inhibitor bound to the enzyme relative to the free enzyme (Jordan *et al.*, 1990).

2.3. Trypsin crystallization and inhibitor complex preparation

Trigonal microcrystals were initially grown using the hanging-drop method (Wlodawer & Hodgson, 1975) in Linbro culture plates (Gilliland & Davies, 1984). Crystallization reservoirs contained 1.8–2.0 *M* ammonium sulfate (AS), 50 m*M* Tris–HCl, 10 m*M* $CaCl_2$ pH 7.4. 6 µl of 15 mg ml^{-1} bovine trypsin (Boehringer Mannheim, catalog number 109 827) in 20 m*M* 2-aminobenzimidazole (2-ABI) was added to 6 µl of reservoir. Macroseeding was used to grow large crystals (Stura & Wilson, 1990). Single crystals were washed in 0.8 *M* AS, 50 m*M* Tris–HCl, 10 m*M* $CaCl_2$ pH 7.4. The washed crystals were placed in a 18 h old hanging drop containing 10 µl of 10 mg ml^{-1} trypsin in 20 m*M* 2-ABI and 10 µl of 1.9 *M* AS, 50 m*M* Tris–HCl, 10 m*M* $CaCl_2$ pH 7.4 (reservoir).

Inhibitor complexes were prepared by soaking the trigonal crystals in inhibitors as follows. Sitting drops containing 10 µl of 5–7 mg ml^{-1} trypsin in water and 10 µl of reservoir (1.9–2.4 *M* AS, 50 m*M* Tris–HCl, 10 m*M* $CaCl_2$ pH 7.4) were prepared. 1 h after the hanging drop was prepared, solid inhibitor was added to the hanging drop. 3 d later, single crystals were washed in 1.6 *M* ammonium sulfite, 50 m*M* Tris–HCl, 10 m*M* $CaCl_2$ pH 7.4 and were then transferred to the hanging drop with the solid inhibitor. Crystals were allowed to soak for a minimum of three weeks.

Bode *et al.* (1990) and Bartunik *et al.* (1989) have described the crystallization of the orthorhombic form of bovine trypsin. Crystals were seeding into drops containing 40 mg ml^{-1} bovine trypsin, 12.5 m*M* benzamidine, 0.7–0.9 *M* AS, 50 m*M* MES pH 6.0, 2.5 m*M* $CaCl_2$, after equilibration against the crystallization reservoir for 1 d. The crystallization reservoirs contained 1.4–1.8 *M* AS, 100 m*M* MES pH 6.0, 5 m*M* $CaCl_2$.

Table 1
Overall statistics of data processing.

Statistics for the highest resolution shell of data are shown in parentheses.

	2-ABI	(I)	(II)	(III)	(IV)	(V)
Space group	$P3_121$	$P3_121$	$P3_121$	$P3_121$	$P3_121$	$P2_12_12_1$
Unit-cell dimensions (Å)						
a	55.02	55.02	54.51	55.02	55.02	63.16
b	55.02	55.02	54.51	55.02	55.02	63.78
c	109.14	109.14	108.71	109.14	109.14	69.35
Reflections	16893	10983	15600	15745	17721	26263
Resolution range (Å)						
High	1.80 (1.80)	1.80 (1.80)	1.80 (1.80)	1.80 (1.80)	1.80 (1.80)	1.80 (1.80)
Low	10.0 (1.90)	10.0 (2.10)	10.0 (2.10)	10.0 (1.90)	10.0 (1.90)	10.0 (1.90)
Completeness (%)	91.1 (78.5)	95.4 (95.0)	67.2 (71.4)	84.5 (68.2)	95.2 (90.0)	99.0 (99.9)
Redundancy	6.3 (4.0)	2.6 (2.0)	2.8 (1.8)	4.5 (2.0)	7.4 (5.1)	3.4
R_{sym}†	0.095 (0.262)	0.098 (0.202)	0.094 (0.175)	0.102 (0.235)	0.075 (0.226)	0.078 (0.222)
Mean $I/\sigma(I)$	8.1 (2.2)	7.6 (3.0)	7.9 (3.7)	6.2 (1.8)	9.7 (2.4)	16.2 (3.1)

† $R_{sym} = |I - \langle I\rangle|/I$.

Orthorhombic trypsin–(V) complex crystals were prepared by transferring crystals to 20 µl sitting drops containing solid (V) in 2.5 mg ml^{-1} bovine trypsin, 0.8–0.9 *M* AS, 100 m*M* MES pH 6.0, 12.5 m*M* $CaCl_2$. Prior to transfer, single crystals were washed in 2.0 *M* AS, 100 m*M* MES pH 6.0, 10 m*M* $CaCl_2$. Crystals were soaked for approximately 16 d prior to being mounted for data collection.

2.4. Crystallographic data collection

Crystals were shipped using crystal shipping tubes (Whitlow, 1996) to Molecular Structure Corporation (MSC) or Area Detector Systems Corporation (ADSC), where 1.8 Å data sets were collected (see Table 1). At MSC, the diffraction data were collected on an R-AXIS II image-plate detector using a Rigaku RU-200 high-brilliance rotating-anode X-ray generator running at 50 kV and 108 mA with a set of MSC/Yale mirrors. At ADSC, the diffraction data were collected on a MAR Research 300 mm image plate on a late-model Siemens high-brilliance rotating-anode X-ray generator with Supper mirrors running at 50 kV and 100 mA. 2θ, the angle between the direct beam and the center of the detector, was 0° and the crystal-to-detector distance was 80–100 mm. Normally, 90° of data were collected in 1.0° frame-widths. One data set was collected with a 0.5° frame-width. Each frame was exposed to X-rays for 10–20 min while the crystal was rotated through a complete frame-width. The X-ray data was processed by Dr Bernard D. Santarsiero at MSC using the *R-AXIS* processing package from MSC and by Dr Xai-Ping Dai at ADSC using the *DENZO* and *SCALEPACK* processing packages (see Table 1 for data-processing statistics).

2.5. Crystallographic structure determination and refinement

The $P3_121$ trypsin–BABCH [2,7-bis(4-amidinobenzylidene)cycloheptan-1-one] complex was prepared and solved by molecular replacement using *X-PLOR* (Brünger, 1993) by Dr Babu at BioCryst Pharmaceuticals Inc. at 2.5 Å resolution to an *R* factor of 26.5%. The unit-cell parameters are $a = 55.02$, $b = 55.02$, $c = 109.14$ Å, $\gamma = 120°$. BABCH is a potent factor Xa inhibitor (Stürzebecher *et al.*, 1989). No temperature factors were used in the refinement and the structure contains no waters. The electron density for BABCH was uninterpretable. Although the $P3_121$ crystal form of trypsin has previously been reported (Bode & Huber, 1978), no coordinates were available in the Protein Data Bank (Bernstein *et al.*, 1977).

The trypsin–BABCH complex was further refined at Berlex Biosciences using *PROFFT*, a restrained-parameter least-squares procedure (Hendrickson, 1985) modified by Finzel (1987) to incorporate the fast Fourier algorithms of Ten Eyck and Agarwal (Agarwal, 1978, 1980). At an *R* factor of 22.3% at 2.0 Å resolution, the trypsin–BABCH complex structure was used as a starting structure for the trypsin–2-ABI complex structure. We are not reporting the trypsin–BABCH complex structure, owing to the difficulty of interpreting the conformation of BABCH in trypsin. The trypsin–2-ABI complex was refined to 1.8 Å resolution to an *R* factor of 17.2% (PDB entry 1qa0). The trypsin structures complexed with (I)–(IV) all used the trypsin–2-ABI complex as a starting model and were all obtained using *PROFFT*. The orthorhombic trypsin–(V) complex used the trypsin DX-9065a as a starting model (Stubbs *et al.*, 1995). Final refinement of all the models was performed using *PROFFT* (Finzel, 1987; see Table 2). R_{free} calculations were performed using 4% of the data not included in the refinements.

3. Results and discussion

3.1. Structure of (I) bound to trypsin

In our effort to develop an orally active inhibitor of factor Xa, we investigated a lead inhibitor series which exhibited the binding affinity of BABCH without the photochemically induced olefin-isomerization liability (Shaw *et al.*, 1998). The diaryl benzimidazoles and diaryl carbazoles were identified as attractive pharmophores. The crystal structure of bovine trypsin–7-[(6-{[1-(1-iminoethyl)piperidin-4-yl]oxy}-2-methyl-1*H*-benzimidazol-1-yl)methyl]naphthalene-2-carboximidamide

Table 2
Summary of crystallographic refinement.

	Weights	2-ABI	(I)	(II)	(III)	(IV)	(V)
Resolution (Å)		1.80	1.80	1.80	1.80	1.80	1.80
Number of reflections		16893	14976	10544	15103	17000	25213
Measured		16893	14976	10544	15103	17000	25213
Used ($F > 2\sigma$)		16656	14816	10451	14721	16575	21568
R factor†		0.172	0.187	0.176	0.188	0.154	0.183
R_{free}		NU‡	0.224	0.278	0.224	0.217	0.237
Number of solvent molecules		270	161	136	138	170	224
Distances (Å)							
Bonds (1–2)	(0.02)	0.017	0.016	0.016	0.016	0.014	0.016
Angles (1–3)	(0.03)	0.033	0.032	0.034	0.033	0.030	0.030
Intraplanar (1–4)	(0.05)	0.046	0.040	0.043	0.044	0.038	0.044
Planar groups (Å)	(0.02)	0.016	0.014	0.014	0.015	0.014	0.015
Chiral centres (Å^3)	(0.15)	0.167	0.185	0.168	0.158	0.162	0.165
Non-bonding contacts (Å)							
Single torsion	(0.50)	0.167	0.173	0.181	0.178	0.167	0.167
Multiple torsion	(0.50)	0.185	0.180	0.218	0.187	0.171	0.214
Possible hydrogen bonds	(0.50)	0.203	0.261	0.321	0.252	0.222	0.228
Torsion angles (°)							
Planar (ω)	(3.0)	2.6	32.6	2.5	2.6	2.7	3.0
Staggered	(15.0)	17.5	16.6	17.1	17.4	16.9	16.2
Orthonormal	(20.0)	18.3	20.1	19.4	19.1	18.9	21.3
Thermal factors (B) (Å^2)							
Main-chain bond	(2.0)	1.61	1.75	1.74	1.95	1.51	1.63
Main-chain angle	(3.0)	2.06	2.42	2.50	2.48	2.16	2.43
Side-chain bond	(3.0)	2.81	3.21	3.22	3.15	3.02	3.14
Side-chain angle	(4.0)	3.46	4.30	4.22	3.6	4.25	4.55

† R factor = $|F_o - F_c|/F_o$. ‡ Not used.

(I) complex has been refined at 10.0–1.8 Å to an R factor of 18.7% and an R_{free} of 22.4% in space group $P3_121$ (PDB entry 1qbo). The electron-density map for trypsin–(I) was easy to interpret (see Fig. 1*a*). The inhibitor (I) is bound at the active site of trypsin (see Fig. 2*a*) in an L-shaped conformation. This binding mode is similar to the bovine trypsin complexes of BX5633 and DX-9065a (Stubbs *et al.*, 1995; see Fig. 5). The naphthylamidine ring is bound in the S1 pocket, making four hydrogen bonds to Asp189 (177),[1] Ser190 (178) and Gly219 (202) (see Fig. 2*a*). The central benzimidazole ring of (I) sits above the catalytic His57 (46) and makes no contacts with the proteins. The acetimidoylpiperidine ring system binds in an extended conformation in the S4 pocket, defined by Thr98 (86), Leu99 (87), Gln175 (161) and Trp215 (199). The imido N atom (N32) on the acetimidoylpiperidine makes a hydrogen bond to water molecule 474, which is hydrogen bonded to the carbonyl O atoms of residues Thr98 and Gln175 (see Fig. 2*a*).

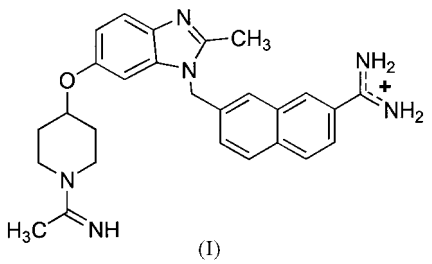

(I)

[1] We will use the chymotrypsin numbering throughout this paper (Bode *et al.*, 1992). Trypsin's numbering will be shown in brackets the first time a residue is cited.

3.2. Structure of (II) bound to trypsin

The crystal structure of bovine trypsin complexed with (II) has been refined at 1.8 Å to an R factor of 17.6% and an R_{free} of 27.8% in space group $P3_121$ (PDB entry 1qb9). (II) is similar to (I). The central carbazole ring system of (II) has an additional fused aromatic ring compared with the central benzimidazole ring system in (I). Knowing the structure of (I) allowed us to interpret the weak electron density of (II) at the active site of trypsin (see Fig. 1*b*). The weak electron density for (II) in this structure is most likely to be a consequence of the incompleteness of this data set (see Table 1) and of the poor aqueous solubility of (II).

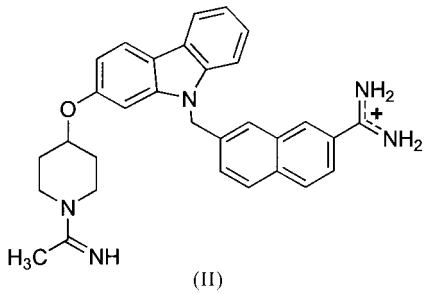

(II)

(II) is bound in an L-shaped conformation very similar to that of (I). The naphthylamidine ring is bound in the S1 pocket, making four hydrogen bonds to Asp189, Ser190 and Gly219 (see Fig. 2*b*). The acetimidoylpiperidine ring system binds in an extended conformation in the S4 pocket. Unlike the (I) complex, the (II) structure does not have water molecule 474, which is hydrogen bonded in the (I) structure to the imido N atom on the acetimidoylpiperidine. This is most

likely to be a consequence of the weak electron density and low occupancy of (II) in the complex.

3.3. Structure of (III) bound in trypsin

The 2,6-diphenoxypyridines were identified as an attractive template without the photochemically induced olefin-isomerization liability of BABCH (Phillips *et al.*, 1998). Structure–activity relationships show that the symmetrical *meta*-substituted bisamidine regioisomers were more potent than other bisamidine analogs. Substitution of fluorines at positions 3 and 5 on the pyridine ring resulted in a twofold to fivefold increase in factor Xa affinity, but did not affect the trypsin affinity (Phillips *et al.*, 1999). 3,3′-[3,5-difluoro-4-methyl-2,6-pyridinediylbis(oxy)] bis(benzenecarboximidamide) (III) has each of these chemical attributes. The factor Xa and trypsin-binding affinities for (III) are 13 and 810 n*M*, respectively. (III) was the first compound to be studied crystallographically.

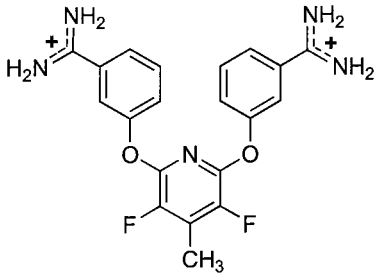

(III)

The crystal structure of bovine trypsin–(III) complex has been refined at 1.8 Å to an *R* factor of 18.8% and an $R_{\rm free}$ of 22.4% in space group $P3_121$ (PDB entry 1qb6). The electron-density map for trypsin–(III) is continuous for the portions of the inhibitor which are in contact with trypsin (see Fig. 3*a*). Little or no electron density was initially found for the solvent-exposed portions. The inhibitor (III) is bound at the active site of trypsin in an L-shaped conformation (see Fig. 4*a*). This binding mode is similar to the bovine trypsin complexes of (I), described above, BX5633 and DX-9065a (Stubbs *et al.*, 1995). One of the two benzylamidine rings is bound in the S1 pocket, making five hydrogen bonds to Asp189, Ser190, Gly219 and a water molecule. The water molecule is hydrogen bonded to the carbonyl O atoms of Trp215 and Val227 (211). The central pyridine ring makes no contacts with trypsin, and the fluorines of (III) are exposed to solvent. The twofold to fivefold affinity increase associated with the fluorine substitutions cannot be explained by the binding of this compound to trypsin. The second benzylamidine ring system binds in the S4 pocket made up of residues Thr98, Leu99, Gln175 and Trp215 in an extended conformation. One of the amidine N atoms makes a hydrogen bond to the carbonyl O atom of Thr98. The electron density for the second benzylamidine is asymmetrical. The occupancies for the ring atoms which are exposed to solvent (C12, C13 and C14) have been lowered to 0.5, owing to the weak electron density around these atoms. This suggests that the second benzylamidine ring is loosely bound to the surface of trypsin. This is consistent with the solid-state double rotational-echo double-resonance NMR (REDOR) results (McDowell *et al.*, 1999).

The REDOR results of (III) bound to trypsin are in overall agreement with the

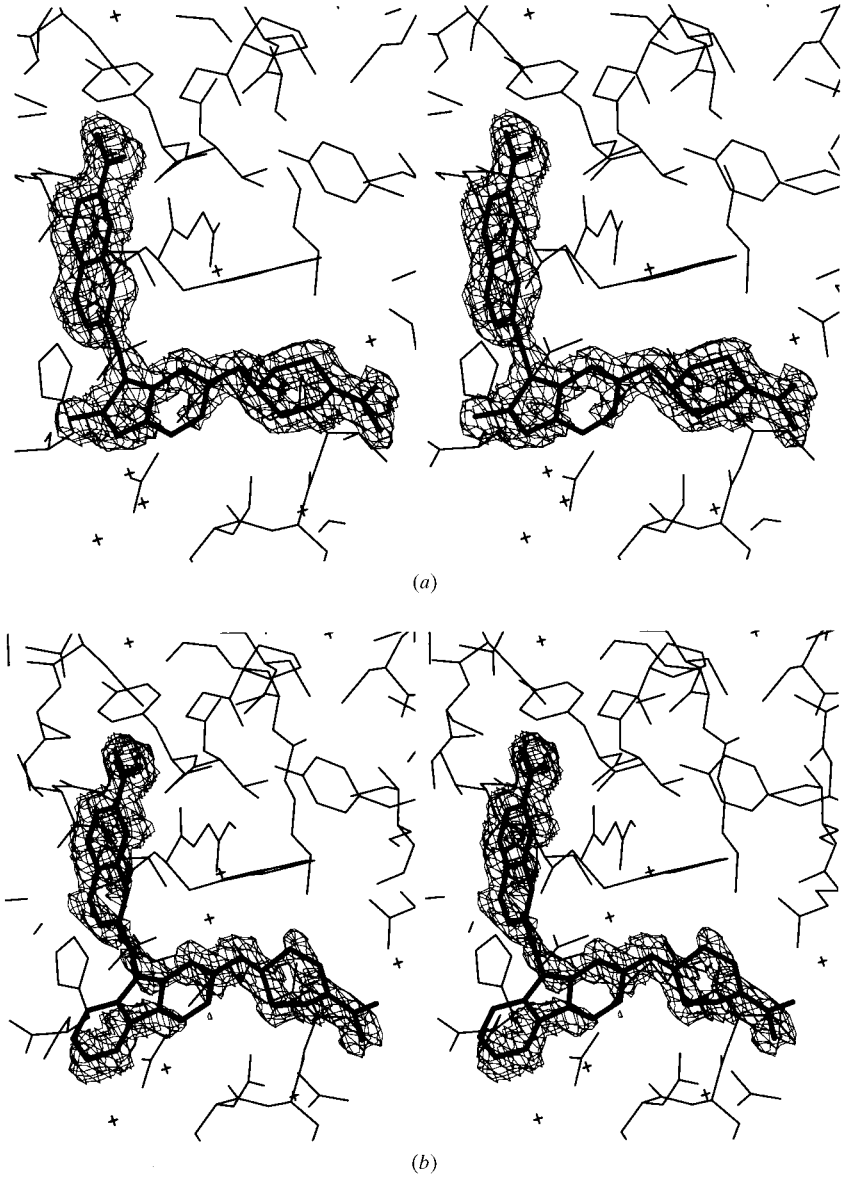

(*a*)

(*b*)

Figure 1
Electron density around (*a*) (I) and (*b*) (II) in bovine trypsin. The $2F_o - F_c$ electron-density maps are displayed at 0.8σ and 0.5σ for (I) and (II), respectively. These figures were produced using the Blob option in *XtalView* (McGee, 1992) with minor editing in Adobe *Photoshop*.

X-ray crystallographic results described above (McDowell *et al.*, 1999). The binding of the second benzylamidine ring system in the S4 pocket is slightly different in the REDOR structure. When the REDOR conformation of (III) is refined against the crystallographic data, the resulting conformation has two bad contacts. C13 in the second benzylamidine and F3 in (III) are 2.57 and 2.53 Å away from CB of Ser127 (114) and CB of Cys128 (115) of a symmetry-related trypsin molecule, respectively. Interestingly, a simple energy minimization of the X-ray structure shifts the second benzylamidine so that it forms an additional hydrogen bond to the carbonyl O atom of Asn97, consistent with the hydrogen bonding of the REDOR structure. This suggests that the conformation of (III) is slightly affected by the packing of a symmetry-related trypsin molecule.

3.4. Structure of (IV) bound to trypsin

The crystal structure of bovine trypsin complexed with 2-{5-[amino(imino)methyl]-2-hydroxyphenoxy}-6-[3-(4,5-dihydro-1*H*-imidazol-2-yl)phenoxy]pyridine-4-carboxylic acid (IV) has been refined at 1.8 Å to an *R* factor of 15.5% and an $R_{\rm free}$ of 21.7% in space group $P3_121$ (PDB entry 1qbn). The electron-density map for trypsin–(IV) was easy to interpret (see Fig. 4*b*). This may be because of the hydrogen bond between the carboxyl group at position 4 on the pyridine ring and the NZ of Lys230 (214) in a symmetry-related trypsin molecule. The inhibitor (IV) is bound at the active site of trypsin in an L-shaped conformation, similar to the (III)-binding mode above (see Fig. 4*a*). The benzylamidine ring is bound in the S1 pocket, making five hydrogen bonds to Asp189, Ser190, Gly219 and a water molecule. The hydroxyl group *para* to the amidine is also hydrogen bonded to a water molecule, which in turn is hydrogen bonded to the hydroxyl group of Ser195 in the catalytic triad. The pyridine ring has no interactions with the primary trypsin molecule. The phenylimidazoline moiety binds in the S4 pocket in an extended conformation. One of the imidazoline N atoms makes a long hydrogen bond to the carbonyl O atom of Asn97 (85).

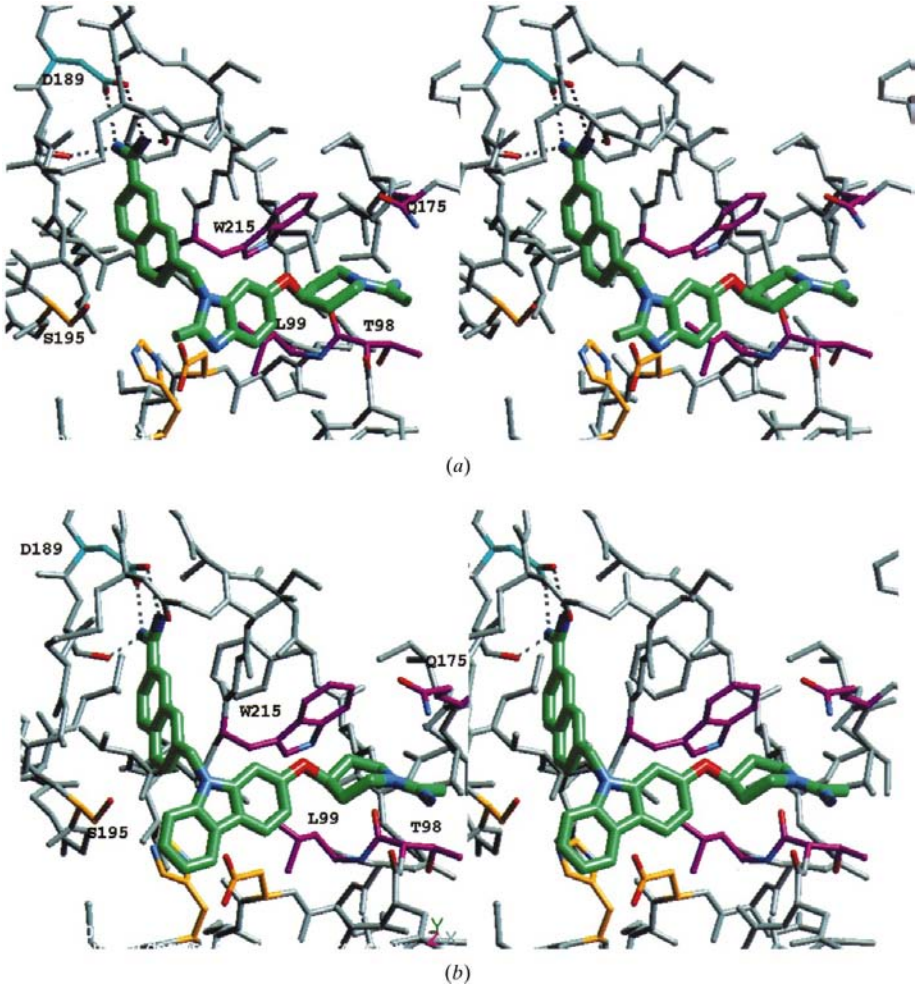

Figure 2
Stereoviews of (*a*) (I) and (*b*) (II) bound in bovine trypsin. The C atoms of the inhibitors are colored green. C atoms of specific residues have been colored. Asp189 (177) at the bottom of the S1 pocket is light blue. The catalytic triad Ser195 (183), His57 (46) and Asp102 (90) are colored orange. Residues which form the S4 pocket, Thr 98 (86), Leu99 (87), Gln175 (161) and Trp215 (199), are colored purple. Hydrogen bonds are depicted as dashed lines.

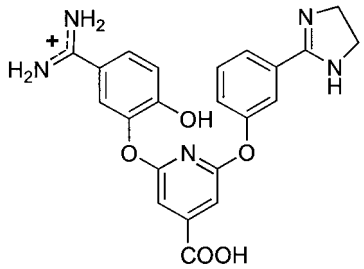

(IV)

The factor Xa and trypsin-binding affinities of (IV) are 85 and 1400 n*M*, respectively (see Table 3). There are four changes in (IV) when compared with (III) above. First, a 6-hydroxyl moiety has been added to the proximal benzylamidine ring. The 6-hydroxyl addition increases the factor Xa affinity of compounds in this series by tenfold to 70-fold and the trypsin affinity by only twofold. In the trypsin–(IV) complex described above, the 6-hydroxyl is hydrogen bonded to a water molecule, which in turn is hydrogen bonded to Ser195 O^{γ} of trypsin. The distance between the 6-hydroxyl and the O^{γ} of Ser195 is only 3.61 Å. We postulate that in factor Xa the 6-hydroxyl would make a direct hydrogen bond to Ser195, in order to account for the affinity increase seen between factor Xa and trypsin. Second, the fluorine substitutions at the 3 and 5 positions on the pyridine ring have been removed, reducing the factor Xa affinity by

twofold to fivefold. Third, the methyl in the 4-position on the pyridine ring was replaced with a carboxylate. This substitution had no significant effect on factor Xa or trypsin binding. Finally, the amidine on the second benzylamidine has been replaced by an imidazoline ring. The amidine to imidazoline substitution in this series reduces the binding affinity to factor Xa by approximately 15-fold, but only reduces the trypsin binding affinity by approximately twofold. Both the amidine in (III) and the imidazoline in (IV) make hydrogen bonds to carboxyl O atoms in trypsin.

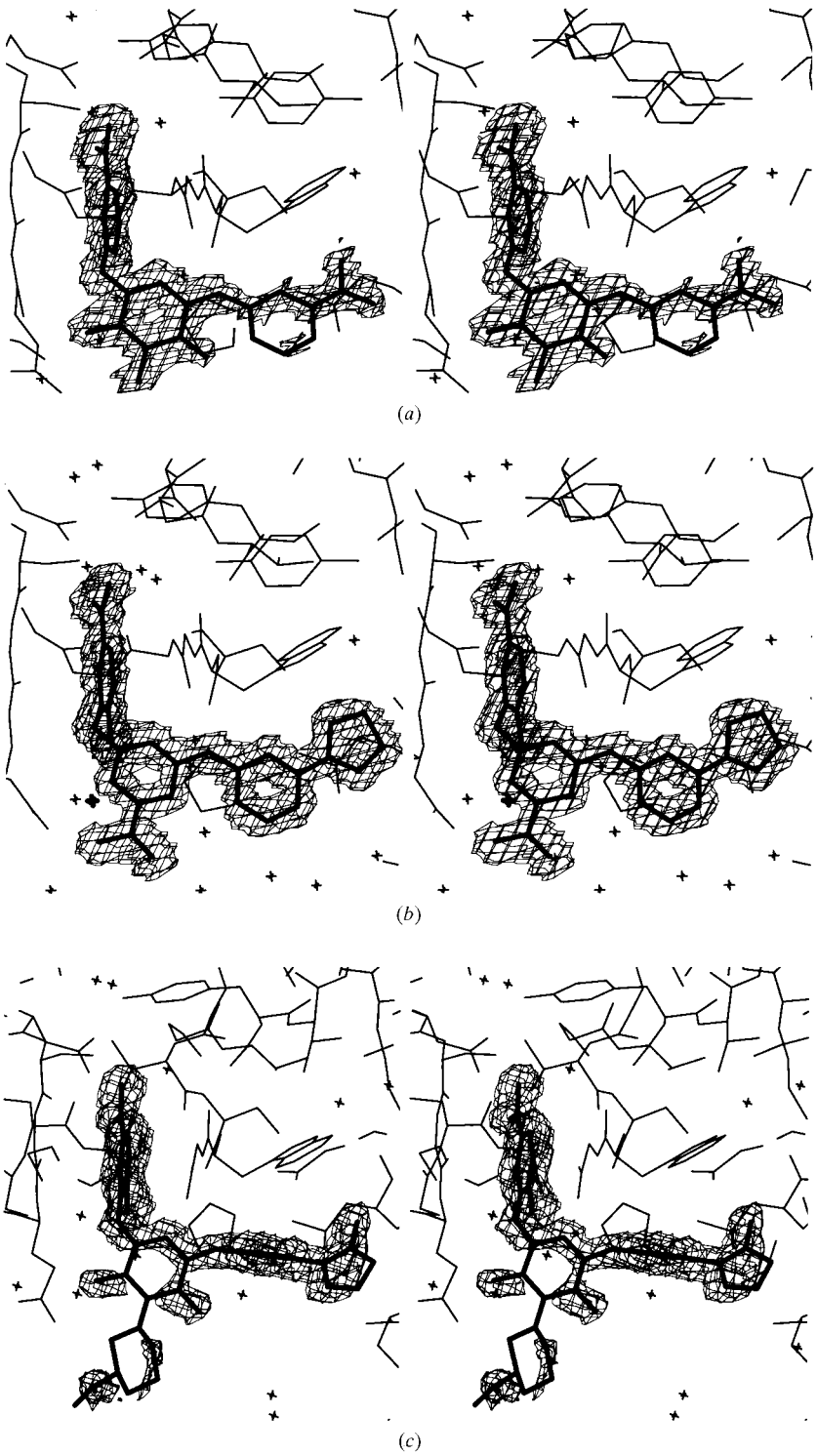

Figure 3
Electron density around (*a*) (III), (*b*) (IV) and (*c*) (V) in bovine trypsin. The $2F_o - F_c$ electron-density maps are displayed at 0.8σ, 1.0σ and 0.8σ for (III), (IV) and (II), respectively. These figures were produced using the Blob option in *XtalView* (McGee, 1992) with minor editing in Adobe *Photoshop*.

3.5. Structure of (V) bound to trypsin

The crystal structure of bovine trypsin 1-(2-{5-[amino(imino)methyl]-2-hydroxyphenoxy}-6-[3-(4,5-dihydro-1-methyl-1*H*-imidazol-2-yl)-phenoxy]pyridin-4-yl)piperidine-3-carboxylic acid (V) complex was refined at 1.6 Å to an *R* factor of 18.6% and an $R_{\rm free}$ of 23.6% in space group $P2_12_12_1$ (PDB entry 1qb1). (V) is bound at the active site of trypsin in an L-shaped conformation, like DX-9065a and the other compounds described above (see Fig. 4*c*). The benzylamidine ring is bound in the S1 pocket, making five hydrogen bonds to Asp189, Ser190, Gly219 and a water molecule. The water molecule is hydrogen bonded to the carbonyl O atoms of Trp215 and Val227. The hydroxyl group *para* to the amidine on the benzylamidine ring is hydrogen bonded to two water molecules, which are in turn hydrogen bonded to the hydroxyl group of catalytic triad Ser195 and the imidazole N atom of His57 in the catalytic triad. The nipecotic acid ring system at position 4 on the pyridine ring has no electron density (see Fig. 3*c*). The 1-methyl-2-(2*H*)-imidazoline ring system binds in the S4 pocket in an extended conformation. The van der Waals radii of two C atoms in the methyl-imidazoline ring and the carboxyl O atom of Thr98 overlap.

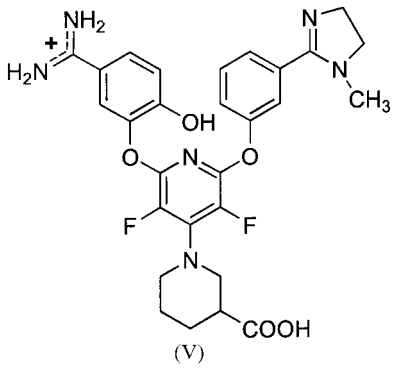

(V)

The factor Xa and trypsin-binding affinities of (V) are 0.11 and 165 n*M*, respectively (see Table 3). There are three changes in (V) when compared to (IV) above. First, the nipecotic acid ring system has been substituted for the carboxylate at position 4 on the pyridine ring. This substitution increases the factor Xa affinity by twofold to fivefold and has little

effect on the trypsin-binding affinity. Second, the fluorine substitutions at the 3 and 5 positions on the pyridine ring have been reintroduced, increasing the factor Xa affinity by twofold to fivefold. Third, the imidazoline ring on the second phenyl has a methyl at the 1-position. This methyl substitution results in a 35-fold increase in the factor Xa affinity and a sixfold increase in the trypsin affinity. The 1-methyl imidazoline ring has a significantly different conformation to the imidazoline ring in (IV) (see Fig. 4*c*). The 1-methyl imidazoline ring does not make a hydrogen bond to trypsin, whereas the imidazoline ring does. The imidazoline in (IV) is coplanar with the attached (distal) phenyl ring, whereas the 1-methyl imidazoline ring in (V) is almost perpendicular to the attached (distal) phenyl ring, having a torsion angle of −52°. The 1-methyl imidazoline lies against Trp215, whereas the imidazoline ring is stacked perpendicular to the Trp215. This increased hydrophobic interaction for the 1-methyl imidazoline ring more than compensates for the loss of a hydrogen bond in the imidazoline ring to trypsin.

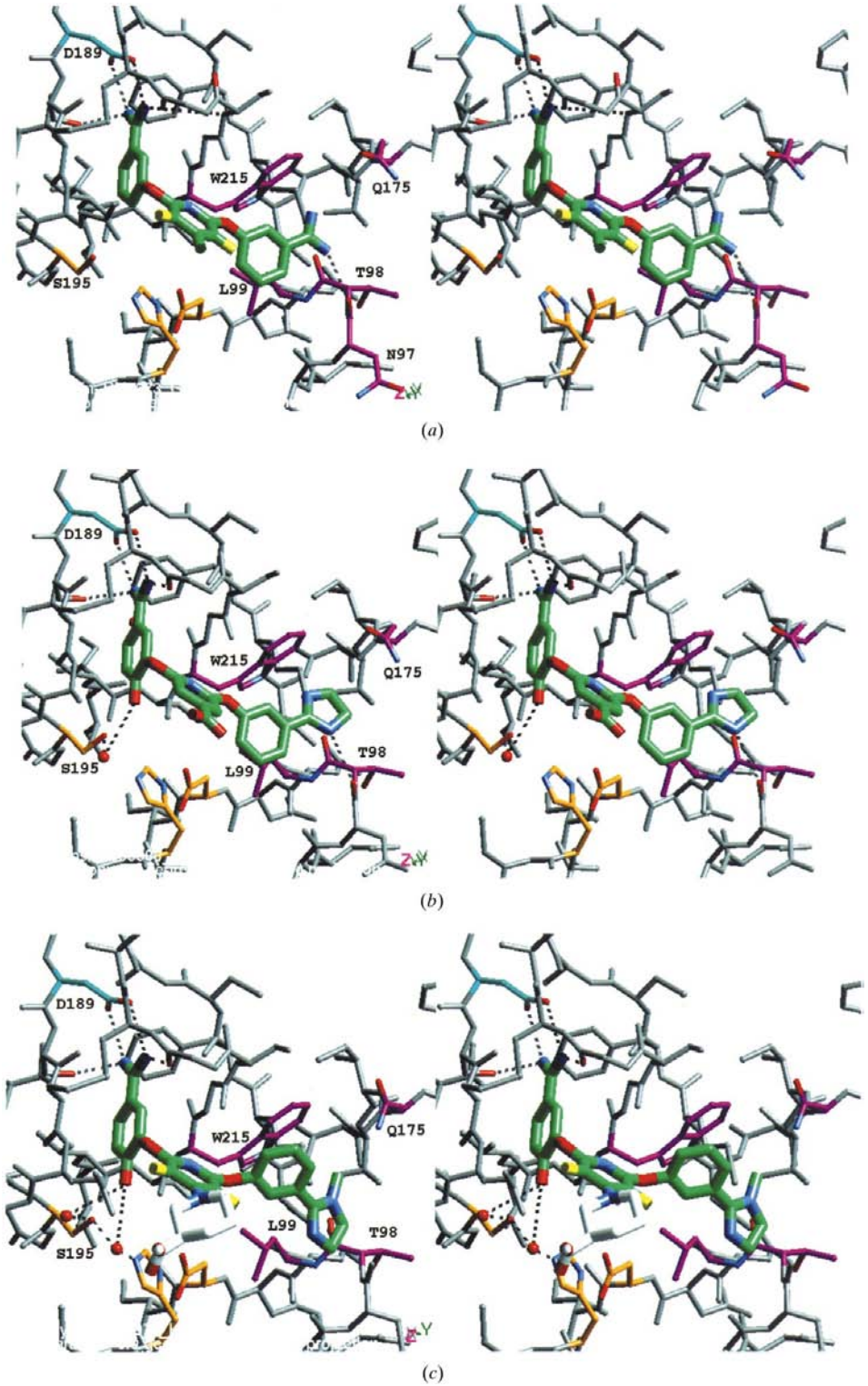

Figure 4
Stereoviews of (*a*) (III), (*b*) (IV) and (*c*) (V) bound in bovine trypsin. The C atoms of the inhibitors are colored green. C atoms of specific residues have been colored. Asp189 (177) at the bottom of the S1 pocket is colored light blue. The catalytic triad Ser195 (183), His57 (46) and Asp102 (90) are colored orange. Residues which form the S4 pocket, Thr98 (86), Leu99 (87), Gln175 (161) and Trp215 (199), are colored purple. Hydrogen bonds are depicted as dashed lines.

The factor Xa inhibitors described in this paper have been crystallographically studied in bovine trypsin and appear to bind to trypsin in a similar manner. The binding is independent of the space group in which they were crystallized, despite close contacts with a symmetry-related trypsin molecule affecting compound binding in the S4 pocket in the $P3_121$ space group. These compounds have several common features. At neutral pH, most of these compounds have two positive charges. One of the positive charged moieties, normally an arylamidine, is involved in a salt bridge in the S1 pocket to Asp189. The second positively charged moiety binds in the S4 pocket, defined by the hydrophobic interactions of Leu99 and Trp215 and the electrostatic interactions of carbonyl O atoms of Ser96 (84), Asn97 and Thr98 and Gln175 OE1.

4. Conclusions

The active sites of bovine trypsin and human factor Xa are very similar, suggesting that the structure–activity relationship and

Table 3
Binding constants and selectivity data for factor Xa inhibitors.

Compounds	K_i (nM)		Selectivity, Trypsin/factor Xa
	Factor Xa	Trypsin	
(*Z*,*Z*)-BABCH	0.66	33	50
Pyridine template			
(III)	14	870	62
(IV)	85	1400	17
(V)	0.11	170	1500
Naphthylamidine template			
DX-9650a	20	200	10
(II)	1.6	36	23
(I)	0.27	18	67

conformations of inhibitors bound to trypsin could be useful in understanding their structure–activity relationship in factor Xa. Renatus *et al.* (1998) have recently come to a similar conclusion. In addition, for the factor Xa inhibitor DX-9065a, the only inhibitor for which complexes have been solved in both bovine trypsin and human factor Xa, the conformation of DX-9065a is very similar in both complexes (Stubbs *et al.*, 1995; Brandstetter *et al.*, 1996). There are five amino-acid changes worth noting between bovine trypsin and human factor Xa (see Fig. 6). One of the common features of our compounds is that they have two positively charged groups; therefore, electrostatic differents are important in understanding the structure–activity relationship of our compounds. The active site of factor Xa has two more negatively charged amino acids than trypsin (Asn97→Asp and Ser217→Glu). Asn/Asp97 is just outside of the S4 pocket and Ser/Glu217 is outside the S3 pocket. Amino-acid changes around the S4 pocket are likely to affect a compound's binding and affinity and hence its selectivity between factor Xa and trypsin. In the hydrophobic S4 pocket, Leu99 is a Tyr in factor Xa and, on other side, the position occupied by Gln175 in trypsin is occupied by Phe174 in factor Xa. One other position is worth noting: in the S1 pocket Ser190 in trypsin is an Ala in factor Xa, making the S1 pocket of factor Xa more hydrophobic.

We believe that there are two possible conformations for the binding of our potent inhibitors to factor Xa. The first possible conformation is that these compounds bind in factor Xa the same way as they bind in bovine trypsin (with the arylamidine binding in the S1 pocket and the second positively charged moiety binding in the S4 pocket in an L-shaped conformation). This is the case for DX-9065a. We favor this possible binding conformation for the naphthylamidine series of compounds, such as (I) and (II). Both (I) and (II) show a very similar binding mode to that reported for DX-9065a in bovine trypsin (see Fig. 5). Despite the differences in the linkers between the naphthylamidine and pyrrolidine/piperidine rings, we expect that the factor Xa binding mode will be essentially the same. A second possible binding mode was

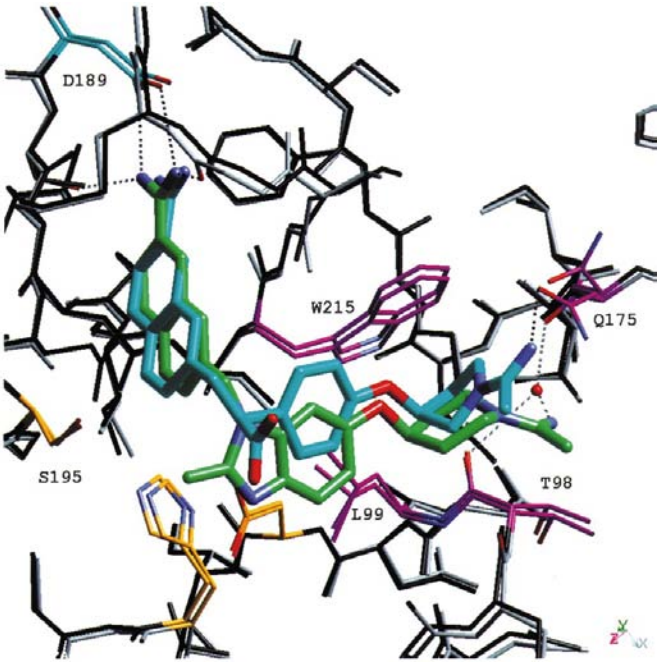

Figure 5
Superposition of bovine trypsin (I) and Daiichi's DX-9065a (PDB entry 1mtw) complexes. The C atoms of the inhibitor (I) and DX-9065a are colored green and blue, respectively. The majority of the C atoms in the trypsin bound to (I) are gray and those bound to DX-9065a are black. C atoms of specific residues have been colored. Asp189 (177) at the bottom of the S1 pocket is colored light blue. The catalytic triad Ser195 (183), His57 (46) and Asp102 (90), are colored orange. Residues which form the S4 pocket, Thr98 (86), Leu99 (87), Gln175 (161) and Trp215 (199), are colored purple. Hydrogen bonds are depicted as dashed lines. Hydrogen bonds to the naphthylamidine in DX-9065a have been omitted for clarity, as they are identical in both complexes.

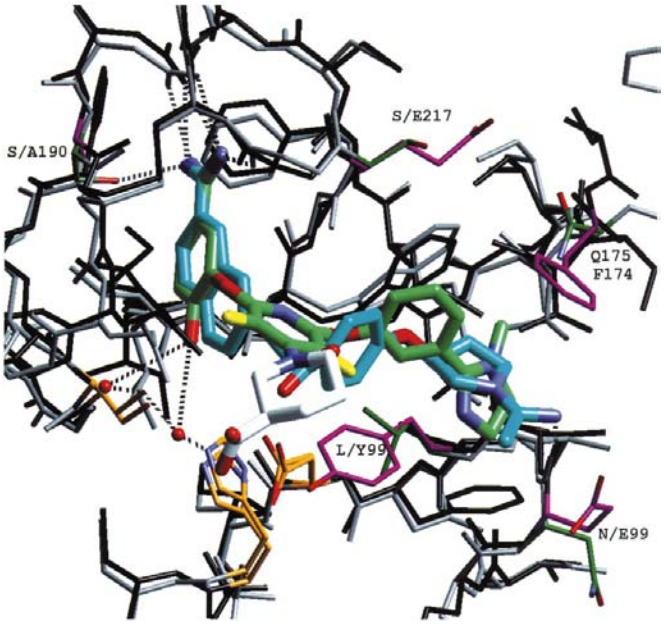

Figure 6
Superposition of the bovine trypsin (V) and human factor Xa DX-9065a (PDB entry 1fax) complexes. The C atoms of the inhibitor (V) and DX-9065a are colored green and blue, respectively. The majority of the C atoms in trypsin are colored gray and in factor Xa are colored black. C atoms of the five amino-acid changes between bovine trypsin and human factor Xa (Asn/Asp97, Tyr/Leu99, Gln175/Phe174, Ser/Ala190 and Ser/Glu217) have been colored green in trypsin and purple in human factor Xa. The catalytic triad residues (Ser195, His57 and Asp102) in both structures are colored orange.

suggested by our modeling studies of BABCH (Shaw *et al.*, 1998). We determined that the active form of BABCH was the *Z*,*Z* regioisomer, which adopts a U-shaped conformation. Instead of the second positively charged moiety interacting with Glu97 as in the DX-9065a complex, it could interact with Glu217 (see Fig. 6). Since the diaryloxypyridines were designed to mimic BABCH, both binding conformations are possible. Crystal structures of these compounds in factor Xa are needed to resolve their binding modes.

We would like to thank Dr Babu at BioCryst Pharmaceuticals Inc. for the initial molecular-replacement solution of the trigonal form of trypsin; Dr Milton Stubbs at the Max-Planck-Institut in München for the seed crystals of the orthorhombic form of trypsin; Dr Bernard D. Santarsiero at MSC and Dr Xai-Ping Dai at ADSC for processing the crystallographic data; Drs Margaret McCarrick and John Morser.

References

Agarwal, R. C. (1978). *Acta Cryst.* A**34**, 791–809.
Agarwal, R. C. (1980). *Refinement of Protein Structures. Proceedings of the CCP4 Study Weekend*, edited by P. A. Machin, J. W. Campbell & M. Elder, pp. 24–28. Warrington: Daresbury Laboratory.
Arnaiz, D. O., Chou, Y. L., Mohan, R., Zhao, Z., Liang, A., Trinh, L., Hinchman, J., Post, J. & Shaw, K. J. (1998). Am. Chem. Soc. Natl Meet., Dallas, Texas, USA, Abstract 128.
Bartunik, H. D., Summers, L. J. & Bartsh, H. H. (1989). *J. Mol. Biol.* **210**, 813–828.
Bernstein, F. C., Koetzle, T. F., Williams, G. J., Meyer, E. F. Jr, Brice, M. D., Rodgers, J. R., Kennard, O., Shimanouchi, T. & Tsumi, M. (1977). *J. Biol. Chem.* **265**, 18615–18620.
Bode, W. & Huber, R. (1978). *FEBS Lett.* **90**, 265–269.
Bode, W. Turk, D. & Karshikov, A. (1992). *Protein Sci.* **1**, 426–471.
Bode, W., Turk, D. & Stürzebacher, J. (1990). *Eur. J. Biochem.* **193**, 173–182.
Brandstetter, H., Kuhne, A., Bode, W., Huber, R., von der Saal, W., Wirthensohn, K. & Engh, R. A. (1996). *J. Biol. Chem.* **271**, 29988–29992.
Brünger, A. (1993). *X-PLOR: A System for X-ray Crystallography and NMR, Version* 3.1. New Haven: Yale University Press.
Davie, E. W., Fujikawa, K. & Kisiel, W. (1991). *Biochemistry*, **30**, 10363–10370.
Finzel, B. C. (1987). *J. Appl. Cryst.* **20**, 53–55.
Griedel, B. D., Arnaiz, D. O., Sakata, S. T., Shaw, K. J., Zhao, Z., Dallas, J., Koovakkat, S., Whitlow, M., Liang, A., Trinh, L., Hinchman, J., Post, J., Ho, E., Subramanyam, B., Vergona, R., Walters, W., White, K., Sullivan, M. E. & Morrissey, M. M. (1998). Am. Chem. Soc. Natl Meet., Dallas, Texas, USA, Abstract 129.
Gilliland, G. L. & Davies, D. R. (1984). *Methods Enzymol.* **104**, 370–381.
Hendrickson, W. A. (1985). *Methods Enzymol.* **115**, 252–270.
Jordan, S. P., Waxman, L., Smith, D. E. & Vlasuk, G. P. (1990). *Biochemistry*, **29**, 11095–11100.
Kamata, K., Kawamoto, H., Honma, T., Iwama, T. & Kim, S.-H. (1998). *Proc. Natl Acad. Sci USA*, **95**, 6630–6635.
Lottenberg, R., Christensen, U., Jackson, C. M. & Coleman, P. L. (1981). *Methods Enzymol.* **80**, 341–361.
McDowell, L. M., McCarrick, M. A., Studelska, D. R., Guilford, W. J., Arnaiz, D., Dallas, J. L., Light, D. R., Whitlow, M. & Schaefer, J. (1999). Submitted.
McGee, D. E. (1992). *J. Mol. Graph.* **10**, 44–46.
Morrison, J. F. (1969). *Biochim. Biophys. Acta*, **185**, 269–286.
Padmanabhan, K., Padmanabhan, K. P., Tulinsky, A., Park, C. H., Bode, W., Huber, R., Blankenship, D. T., Cardin, A. D. & Kisiel, W. (1993). *J. Mol. Biol.* **232**, 947–966.
Phillips, G. B., Buckman, B. O., Davey, D. D., Eagen, K. A., Guilford, W. J., Hinchman, J., Ho, E., Koovakkat, S., Liang, A., Light, D. R., Mohan, R., Ng, H. P., Post, J., Smith, D., Subramanyam, B., Sullivan, M. E., Trinh, L., Vergona, R., Walters, J., White, K., Whitlow, M., Wu, S., Xu, W. & Morrissey, M. M. (1998). *J. Med. Chem.* **41**, 3557–3562.
Phillips, G., Davey, D., Eagen, K., Ng, H. P., Pinkerton, M., Koovakkat, S. K., Whitlow, M., Liang, A., Trinh, L. & Morrissey, M. M. (1999). *J. Med. Chem.* **42**, 1749–1756.
Renatus, M., Bode, W., Huber, R., Stürzebecher, J. & Stubbs, M. T. (1998). *J. Med Chem.* **41**, 5445–5456.
Shaw, K. J., Guilford, W. J., Dallas, J. L., Koovakkaat, S. K., McCarrick, M. A., Liang, A., Light, D. R. & Morrissey, M. M. (1998). *J. Med Chem.* **41**, 3552–3556.
Sitko, G. R., Ramjit, D. R., Stabilito, I. I., Lehman, D., Lynch, J. J. & Vlasuk, G. P. (1992). *Circulation*, **85**, 805–815.
Stubbs, M. T., Huber, R. & Bode, W. (1995). *FEBS Lett.* **375**, 103–107.
Stura, E. A. & Wilson, I. A. (1990). *Methods*, **1**, 38–49.
Stürzebecher, J., Stürzebecher, U., Vieweg, H., Wagner, G., Hauptmann, J. & Markwardt, F. (1989). *Thromb. Res.* **54**, 245–252.
Whitlow, M. (1996). *J. Appl. Cryst.* **29**, 204–205.
Wlodawer, A. & Hodgson, K. O. (1975). *Proc. Natl Acad. Sci. USA*, **72**, 398–399.